Research Article | Vol. 26, No. 22 | 29 Oct 2018 | OPTICS EXPRESS 28323

Optics EXPRESS

Automated precision alignment of optical components for hydroxide catalysis bonding

DAVID I. ROBERTSON,[1,*] EWAN D FITZSIMONS,[2] CHRISTIAN J. KILLOW,[1] MICHAEL PERREUR-LLOYD,[1] AND HENRY WARD[1]

[1] *SUPA, School of Physics and Astronomy, University of Glasgow, Glasgow G12 8QQ, Scotland, UK*
[2] *UK Astronomy Technology Centre, Science and Technology Facilities Council, Royal Observatory Edinburgh, Edinburgh EH9 3HJ, UK*
[*] *david.robertson@glasgow.ac.uk*

Abstract: We describe an interferometric system that can measure the alignment and separation of a polished face of a transparent optical component and an adjacent polished surface. Accuracies achieved are $\sim 1\mu$rad for the relative angles in two orthogonal directions and $\sim 30\mu$m in separation. We describe the use of this readout system to automate the process of hydroxide catalysis bonding of a fused-silica component to a fused-silica baseplate. The complete alignment and bonding sequence was typically achieved in a timescale of a few minutes, followed by an initial cure of 10 minutes. A series of bonds were performed using two fluids - a simple sodium hydroxide solution and a sodium hydroxide solution with some sodium silicate solution added. In each case we achieved final bonded component angular alignment within 10 μrad and position in the critical direction within 4 μm of the planned targets. The small movements of the component during the initial bonding and curing phases were monitored. The bonds made using the sodium silicate mixture achieved their final bonded alignment over a period of ~ 15 hours. Bonds using the simple sodium hydroxide solution achieved their final alignment in a much shorter time of a few minutes. The automated system promises to speed the manufacture of precision-aligned assemblies using hydroxide catalysis bonding by more than an order of magnitude over the more manual approach used to build the optical interferometer at the heart of the recent ESA LISA Pathfinder technology demonstrator mission. This novel approach will be key to the time-efficient and low-risk manufacture of the complex optical systems needed for the forthcoming ESA spaceborne gravitational waves observatory mission, provisionally named LISA.

1. Introduction

Precision-aligned, robust, ultra-stable optical assemblies are required in an increasing number of applications. They have been used in space based applications in areas such as science, metrology and geodesy [1, 2]. One recent example was the optical bench for the European Space Agency LISA Pathfinder mission (LPF) [3, 4] for which specially developed alignment and bonding techniques were used to construct the flight hardware [5]. For LPF, fused-silica optics were hydroxide catalysis bonded [6] to a Zerodur baseplate to form multiple interferometers. The alignment of the interferometers was maintained through build, testing, launch and operations, proving the suitability of the bonding technique for building precision optics for long-term operation in a space environment.

Hydroxide catalysis bonds can achieve high alignment precision and are extremely thin, strong and stable. Once cured the bonds are permanent and are robust against environmental conditions, so do not need special storage, and can be used to cryogenic temperatures (2.5 K). For combinations of these reasons hydroxide catalysis bonding was used in LPF and Gravity Probe-B [1] over other jointing techniques such as e.g. glueing or optical contacting.

The construction of the LPF optical bench and its subsequent in-flight performance were very successful. However, the build phase was rather lengthy and involved a procedure that required

#334474 https://doi.org/10.1364/OE.26.028323
Journal © 2018 Received 26 Jun 2018; revised 12 Sep 2018; accepted 17 Sep 2018; published 16 Oct 2018

Optics EXPRESS

multiple skilled operators. Each bond involved considerable component handling to optimise alignment before bonding. Typically a bond of a single precision-aligned component took around a day to complete.

Looking forward to new applications, there is a clear imperative to speed-up the complete alignment and bonding process while achieving at least as good tolerances as have been demonstrated with the manual technique. To this end we have developed and demonstrated an automated system that incorporates computer-controlled precision measurement and component handling techniques. With this novel system, we can routinely achieve positioning and alignment accuracies of bonded components of $< 4\,\mu$m and $< 10\,\mu$rad, with a bond now taking a single operator around 20 minutes to complete.

In this paper we describe the new automated system and its use to perform a series of sample bonds. The accuracies achieved demonstrate the success of the automated approach.

2. Metrology for hydroxide catalysis bonding

Hydroxide catalysis bonding is an essentially "glueless" technique for permanently bonding a wide variety of glass and ceramic pieces together. The bonding process does not need a filler: the water liberated during the bond curing eventually dissipates leaving the surfaces joined by a new network of covalent bonds. This is a key aspect of the process that results in the strength, excellent stability, and low mechanical loss [6] of the final assembly.

The technique relies on the surfaces to be joined being very clean and closely matched in surface shape. Typically, surfaces to be bonded are flat, for which an appropriate specification is a flatness over the bonding area of 63nm (peak to valley) and an rms roughness of less than 1nm [6]. To form the bond the surfaces are carefully brought together with a very small amount of a weak hydoxide solution placed between them. The hydroxide solution catalyses the bonding of the two surfaces and the bond becomes permanent over a timescale of order minutes, with full strength being achieved over a timescale of days to weeks, depending on material properties and curing temperature.

Achieving high accuracy of position and in-plane angle of a component after bonding is completed depends on a number of factors. Of particular importance is the manner in which the two surfaces are brought together once the bonding fluid has been applied. Significant lack of parallelism ($\gtrsim 10\,\mu$rad) of the surfaces can readily result in slight slippage of the component and hence inaccuracy of its final bonded alignment. Therefore an ideal system should be able to monitor and optimise the relative surface alignment as the component is lowered towards contact with the bonding fluid. A monitor of the separation of the surfaces is also desirable to allow full automation of the process.

2.1. Coordinate system adopted

To aid the discussion of the alignments involved in a typical bonding process we define a right-handed coordinate system based on the desired target position and alignment of the component on the baseplate (Fig. 1). The coordinate origin is at the planned reflection point on the front surface of the component, the X-axis lies normal to the front surface of the component and in the plane of the baseplate, the Y-axis lies in the plane of the baseplate and is aligned along the front face of the component, and the Z-axis is normal to the baseplate and hence also lies in the plane of the front surface of the component.

With reference to the nominal desired component alignment, we denote the in-plane rotation angle error by α, and the in-plane translational offset of the component by X. Two angles decribe the relative parallelism of the bonding surfaces: the out-of-plane tip angle of the component, γ, and, in the orthogonal direction, the tilt angle β. This nomenclature for angles and coordinates is shown in Fig. 1.

Optics EXPRESS

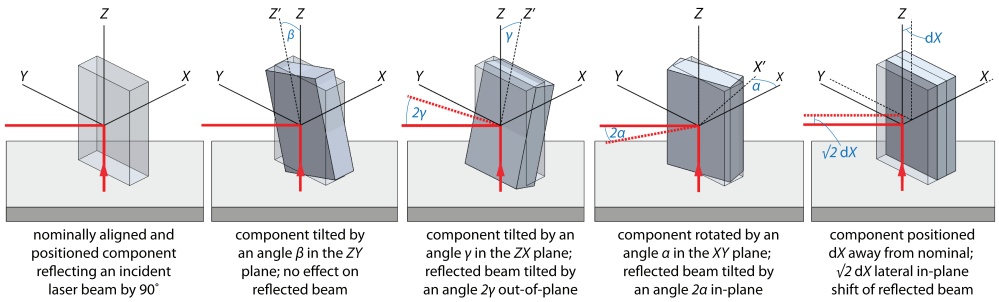

Fig. 1. Sketches of the component in its nominal orientation with the associated XYZ coordinate system, together with illustrations of potential component misalignments and mispositioning and their effect on the reflection of a beam incident in the XY plane at 45 degrees to the nominal component alignment. The solid red lines show the nominal beam path; the dotted red lines show the reflected beam path in each misaligned case.

For critical alignment applications there will normally be a high-resolution measurement of the intended position and angle of the component to be bonded. Often this will come from an optical lever, where a laser beam reflected from the component has to pass through two defined points. This technique was developed within the context of the LPF work [7] and has been shown to provide of order few micron and few tens of microradian targeting of the optical lever beam.

The final out-of-plane angle γ will depend only on the manufacturing tolerance of the component and on uniformity of bond layer thickness. Frequently the angle between optical surface and bonding surface will be nominally 90 degrees. As an example of what can be achieved, in LPF we specified components with face-to-bonding-surface perpendicularity of 1 arcsecond or better, and the resulting out-of-plane beam walk was less than 15 μm after multiple reflections and multiple passes across a 20 cm-scale square baseplate.

With the final γ angle determined by component tolerances, the goal in bonding is to achieve accurate control of the final in-plane angle α and the in-plane location of the component in the X and Y degrees of freedom. Translation in the X direction perpendicular to the component reflecting surface is typically critical, since mispositioning along this axis results in a lateral shift of the reflected optical lever beam. In contrast, translation of the component in the Y direction is parallel to the optical surface and is normally only required to be controlled to the mm level for cm-scale optical components; this can therefore be done without high resolution metrology and is not considered further in this paper.

The challenge during the bonding process is, therefore, to monitor and control with high accuracy α and X and also the three other degrees of freedom, the parallelism and separation of the surfaces to be bonded, that are described by β, γ, and Z.

We discuss these metrology and manipulation aspects in the following sections.

2.2. Component holding and manipulation

Multi-axis manipulation of a component is in principle possible using stacked translation and tilt stages. However a more accurate and convenient solution for our application is to use a 6 degree of freedom hexapod. This was the approach adopted during the LPF OB build for various high precision positioning tasks and is known to produce repeatable and accurate motions at the sub-micron and few-microradian scales. One key attribute of the hexapod used (PI H-824) is the facility for defining in software a pivot point about which the hexapod can be commanded to produce calibrated angular motions. The pivot point is set to the incident point of the optical lever

Optics EXPRESS

beam on the component surface with mm level precision. The iterative nature of the alignment process means that any alignment errors introduced by small offsets in the pivot point quickly become negligible. All hexapod movements are commanded by sending ASCII strings over a serial interface from the computer used to automate the bonding process.

We secure the component in a holder that is attached to a piezo-driven linear actuator (Thorlabs NF15AP25/M) fixed to the end of an aluminium arm that is attached to the moving platform of the hexapod. Figure 2 shows the mounting arrangement. The holder is 3D-printed in ABS

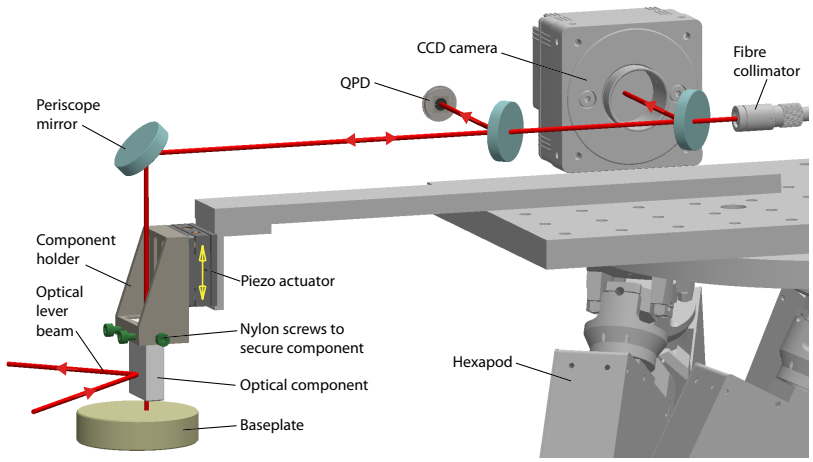

Fig. 2. A sketch of the component suspended from an arm attached to the hexapod. The beam passing vertically through the component is used for the angle and vertical separation metrology (β, γ, Z); the beam reflected from the face of the component is for the optical lever readout of component pointing and positioning (α, X).

plastic and designed to suit the size of the component being bonded. It is readily replaceable if other sizes of components are to be used. The current holder design has internal mechanical registration stops and three threaded holes. The component is inserted against the stops and secured by three nylon screws pressing on the upper part of its surfaces as shown in Figs. 2 and 3. Remote-controlled component clamping and release is under consideration for a future development.

2.3. Bonding surface interferometer

We have developed an interferometric system to measure the relative angular alignment of the bonding surfaces; the measurements provide correction signals to command hexapod angular motions to optimise this alignment as the surfaces are brought together. Our interferometer also provides a signal proportional to the macroscopic separation of the surfaces, allowing rapid automated descent of the component towards the bonding point.

As shown in Fig. 2, the main parts of the interferometer are mounted on the top plate of the hexapod. Laser light from a fibre-coupled diode laser operating at 633nm passes along the hexapod arm and is then reflected to pass vertically through the component towards the bonding surfaces. As illustrated in Fig. 4, the interferometer is formed by optically combining laser light reflected from the bonding face of the component and a coherent beam that is reflected from the surface of the baseplate. Approximately matched fractions of the incident laser intensity are reflected from the two bonding surfaces back along the incoming beam direction and yield high-visibility interference fringes when the surfaces are close to parallel. The component is wedged on its top surface by a (non-critical) $\sim 2^\circ$ angle so that the unwanted reflection from

Optics EXPRESS

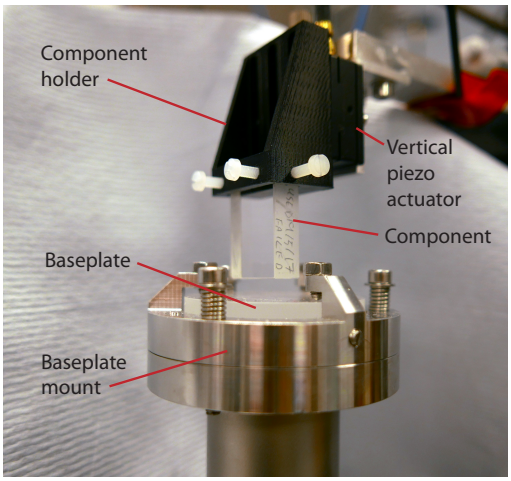

Fig. 3. Detail of the component in its holder. The component (32 mm × 22 mm × 8 mm) held in its black mount by plastic screws. Behind the component holder is the vertical piezo stage which is mounted on an aluminium arm from the hexapod. The component is being held above a circular baseplate.

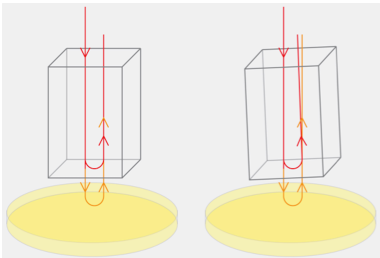

Fig. 4. Sketch showing the laser beams reflected from the bonding surfaces. Left: perfect alignment; right: component misaligned relative to the baseplate. Note that for clarity the incident and return beams are shown spatially separated here; in reality they are essentially collinear.

this surface does not contribute to the interference signal. The returning beams from the two interfaces are split by a beamsplitter, with part directed towards a quadrant photodiode and part towards a CCD camera. The beams incident on the camera are used for initial alignment of the surfaces, which is adjusted by manually commanded hexapod movements to produce satisfactory overlap of the two beams.

2.4. Bonding surfaces: metrology of relative angles

For the readout of the surface parallelism we use an adaptation of the standard technique of differential wavefront sensing [8]. If the bonding surfaces are not parallel, the two interfering beams will have relative wavefront tilt at the point of detection by the quadrant photodetector (QPD). Considering a single dimension for simplicity, a relative wavefront tilt results in a proportional phase difference between the fringe signal detected by one half of the QPD compared with that detected by the other half. We readout the time series from the QPD quadrants, digitising the data streams at 50 kHz. In essentially real time, a computer program analyses the time shifts between combinations of the quadrant signals. To compute the corresponding relative wavefront angles - and hence relative bonding surface angles - the measured time intervals need to be scaled

Optics EXPRESS

by the instantaneous full-fringe timescale. However fringes arising from random acoustic and mechanical disturbance of the setup are unpredictable and very variable in timescale. So we impose a few micron amplitude modulation of the component vertical position by sinusoidal drive at 20 Hz of the piezo actuator, thereby producing clear fringes with characteristic periods that are broadly consistent across a number of fringes. Measurement of the fringe timescales then allows the necessary scaling of the measured QPD phase shifts. The computer analysis program performs vetoing of potentially inaccurate measurements. In particular, the rate of observed fringes has to be within planned bounds and the deduced angles have to be self consistent across measurements made over a number of fringes. Since the measurement relies on analysis of fringes, valid angle readout is achieved provided an air gap remains between the bonding surfaces. With the bonding fluid volume we use, we can continue to achieve angle measurements untill the surface separation is reduced to around 20 microns. The readout scheme provides relative angle measurements in two dimensions (γ and β) with an accuracy of $\sim 1\ \mu$rad, more than sufficient surface alignment for bonding.

2.5. Bonding surfaces: metrology of relative separation

The system described above is essentially an interferometer with what is often termed "internal modulation", where modulation of the relative pathlength of the interferometer arms provides a convenient signal for analysis. To derive a signal proportional to the vertical component-baseplate separation we employ an analogous technique of "external modulation". This technique uses modulation of the laser frequency. If an interferometer has fixed, but unequal arm lengths, such laser frequency modulation results in corresponding movement of the point on the interference fringe seen at the interferometer output. The resulting intensity modulation at the interferometer output at the midpoint of a fringe is proportional to the depth of frequency modulation (which we keep fixed) and, crucially, is proportional to the macroscopic arm length difference.

In our case, the pathlength difference is the round-trip distance between the bottom of the component and the baseplate, which is (twice) the separation that we wish to measure. We modulate the diode laser current at 5 kHz producing a frequency modulation of some tens of GHz. In the sum of the QPD intensity signals we detect the amplitude of the signal component that is coherent with the laser frequency modulation. The vertical component position modulation ensures that there are many fringes available for midpoint measurement of the maximum coherent amplitude.

We calibrate this macroscopic separation readout by stepping the hexapod by a series of known vertical displacements. This process takes about 30 seconds. Our experience is that the laser frequency and frequency modulation amplitude remain sufficiently constant during the time for the calibration and subsequent bonding, that, once calibrated, we can monitor the vertical separation with an uncertainty no worse than 30 μm over a range of 2 cm. This readout allows a rapid automated lowering of the component to close to the point of bonding. A new calibration is performed for each bond.

Once we are ready to bond, a further feature of the interferometer readout system allows detection of when the component being lowered makes contact with the bonding fluid. The number of fringes that are cycled through in one drive cycle of the piezo actuator is monitored. When the component makes contact with the fluid the dynamics of the system change and the motion is damped, resulting in significantly fewer fringes. This change can be detected by the controlling software which can then stop the automated descent. From that point only a few small additional manually commanded hexapod movements are needed to bring the surfaces together.

This level of metrology and automation minimises the time between bonding fluid application and final bonding, avoiding significant bonding fluid evaporation or surface etching.

Software controls the calibration, alignment and controlled descent processes and records all data in a form convenient for anaylsis by a MATLAB script to generate a complete record of the

Optics EXPRESS

bonding process for the component.

2.6. Alignment monitoring

For the demonstration bonds described in this paper we used a twin quadrant-photodiode technique [7] to define and to monitor the pointing of an optical lever beam reflected from the componenent being bonded. The light source for the optical lever was a He-Ne laser operating at 633 nm. Intensity modulation of the beam at a few hundred Hz was provided by passing the the beam through an acousto-optic modulator (AOM) driven by an amplitude modulated *rf* signal. Position measurements were then derived by coherent detection of modulated signals, making the measurements insensitive to low frequency fluctuation of background light levels. From the AOM, the laser light was conducted to the vicinity of the bonding setup by a single-mode optical fibre and was then emitted from a mechanically stable fibre collimator. The beam from the collimator was linearly polarised by passing through a polarising beamsplitter and was then incident on the partially reflecting face of the component being aligned and bonded. The reflected beam was split equally by a beamsplitter, with the resulting beams directed to two position-sensing quadrant photodiodes. One photodiode was placed in close proximity to the beamsplitter and the second photodiode approximately 40 cm further away. A sketch of such a system is shown in Fig. 5. The fibre collimator and all mirrors, beamsplitters and photodiodes were secured to the steel surface of a large optical table.

The four measurements of spot positions on the quadrant detectors yields the four degrees of freedom of the reflected beam vector measured with respect to the nominal line joining the centres of the two detectors. From these data, in the in-plane direction we deduce the beam translation X and angle α; in the out-of-plane direction the translation Z (which is unaffected by the component position and alignment) and angle γ are obtained.

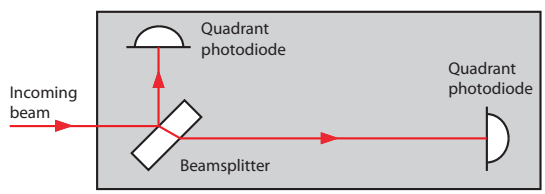

Fig. 5. Sketch showing the concept for monitoring the alignment of the optical lever. The position of the beam is detected on two quadrant photodiodes at different distances from a beamsplitter, allowing the position and direction of the beam to be calculated.

For measurements of more than about 30 minutes duration, slight drifts in the pointing of the input light from the collimator could potentially mimic component movement. To remove this effect the beam transmitted through the component was monitored in the same way as the reflected beam. Any input beam movement seen in this "monitor" was subtracted from the component beam movement to get a reflected beam vector that was independent of input beam pointing for small angular changes. Genuine movement of the component couples in very weakly to the monitor beam pointing and has a negligible effect.

For maximum stability of alignment, care was taken to assemble the system with the minimum number of mirrors in the beam paths to the quadrant detectors.

3. Development of the bonding process

During the initial development of the system, various trial bonds were made using different volumes of bonding fluids, different types of bonding fluid, and different procedures for bringing

Optics EXPRESS

the components together to the point of bonding.

It was found that smaller volumes showed less variability in component angular alignment from initial placement to final cured position. For our test components with rectangular cross-section of size 22 mm by 8 mm, a volume of 0.4μl was found to be just sufficient to wet the whole bonding surface and so this was used for each of the reported test bonds. Given the area of the bonding surface, less chamfers, this corresponds to a fluid volume of $\sim 0.25\mu\mathrm{l/cm}^2$.

After the initial tests, two different bonding fluids were chosen for the final demonstration bonds. The first was the formulation of fluid used for the construction of the LISA Pathfinder optical bench. This was a hydroxide-silicate mixture, consisting of $Na_2O(SiO_2)_x \cdot xH_2O$ which has 27% SiO_2 in 14% NaOH by volume (Sigma-Aldrich 338443). This was then diluted 1 part solution to 6 parts deionised water. We label these bonds as "silicate" bonds. The second fluid was a 0.1mol/l NaOH solution. Bonds made with this solution are labelled as "hydroxide" in the results.

The silicate bonding process is space-proven having flown successfully in both Gravity Probe-B and LPF. The hyroxide process has extremely similar chemistry to the silicate process so we would expect similar strength and stability, but it has not yet been fully tested for space flight. The two processes achieve equal precision in alignment.

The optimised procedure detailed below was followed for all of the test bonds described in this paper.

- The component and baseplate are cleaned and the component is mounted in the holder and the baseplate mounted in a mechanically stable jig.
- Under software control, the component is moved to a height of around 2 mm above the baseplate and an automated alignment sequence performed to make the bonding surface parallel to the baseplate.
- The component is then raised in Z by 10 mm and both bonding surfaces given a final single wipe using high-purity methanol.
- The automated vertical separation readout calibration is performed, ending with the component at a nominal separation of 200 μm from the baseplate. At this point a further automated alignment of bonding surface parallelism is performed, together with a separate automated sequence to align the optical surface – by hexapod adjustment of α and X – so that the reflected optical lever beam is centred on the two monitoring quadrant photodiodes. This is the starting point of the alignment data shown later in Fig. 7 .
- The component is then moved up 10 mm, bonding fluid applied to the baseplate, and the automated sequence started that brings the component down until it touches the bonding fluid.
- The fluid spread causes some vertical angular (γ) misalignment of the optical surface as the bonding fluid pulls the surfaces together. This is a transient effect until the surfaces are fully parallel and the bond cured. The vertical component position modulation is turned off and a further 5 μm downwards step executed. This recovers some of the angular (γ) misalignment. If necessary to optimise the optical lever beam alignment, one or more automated alignments of the optical surface can be applied for up to 70 seconds after the spread of the bonding fluid. The component is then held in place for 12 minutes, without control inputs, to allow the bond to develop.

4. Results

Five test bonds were made using the "silicate" fluid and four using "hydroxide" fluid, and the various data collected and plotted. A summary of the final alignment data for all of the test bonds

Optics EXPRESS

is shown in Fig. 6. All cases showed excellent position and angle of the optical surface after bonding: component X position and α and γ angles were within 4 μm and 10 μrad of the target values in all cases. These results are all well within the current LISA alignment requirements of 15 μm and 17 μrad. There was no significant difference between the final alignment achieved with the two different bonding fluids.

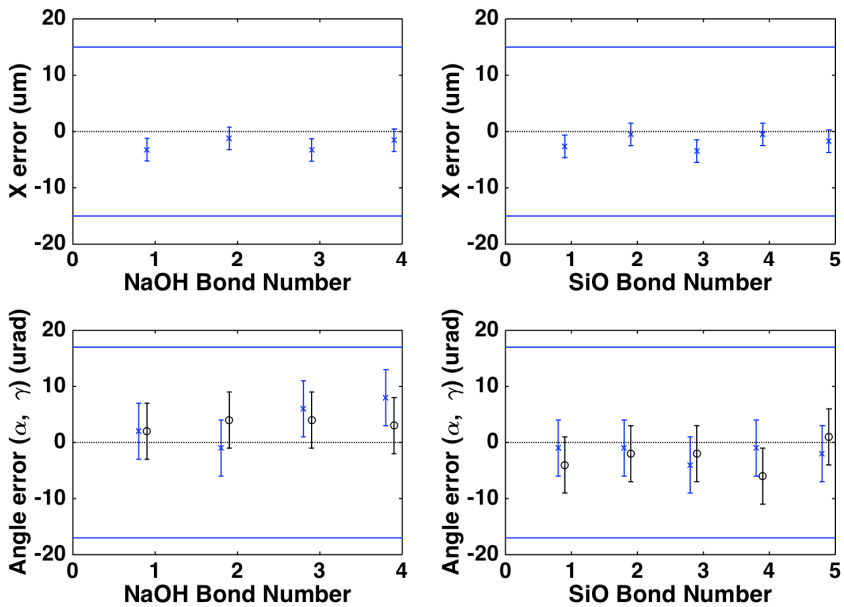

Fig. 6. Final alignments of all of the test optics. Final X position offsets are shown in the top two graphs. In the bottom two graphs the final α angle offsets are shown with blue 'x' data points and final γ angle offsets with black 'o' data points. The solid horizontal lines show the most demanding of the LISA alignment requirements. The vertical error bars indicate measurement uncertainty, largely due to air currents causing fluctuating beam positions.

To illustrate the dynamics of the bonding process we now discuss in more detail one example bond, silicate test bond 5. The alignment data during the bonding process is shown in Fig. 7, with the long term alignment shown in Fig. 8. The various stages of the bonding process are shown on the graph and are detailed in the caption.

The timelines for hydroxide and silicate bonds are essentially identical up to the point that the component clamp is released. After the release of the clamp the hydroxide bonded components reach their final alignment within a few minutes. The silicate bonded components achieve the same precision of final alignment, but only after many hours. This can be seen in Fig. 8 where the final alignment is achieved after around 15 hours.

When assembling complex optical systems with many bonded components there is therefore a potentially significant time saving to be gained by adopting hydroxide bonding. Consequently it is a priority that hydroxide bonds are subjected to a range of strength and environmental tests to establish their suitability for spaceflight use.

Optics EXPRESS

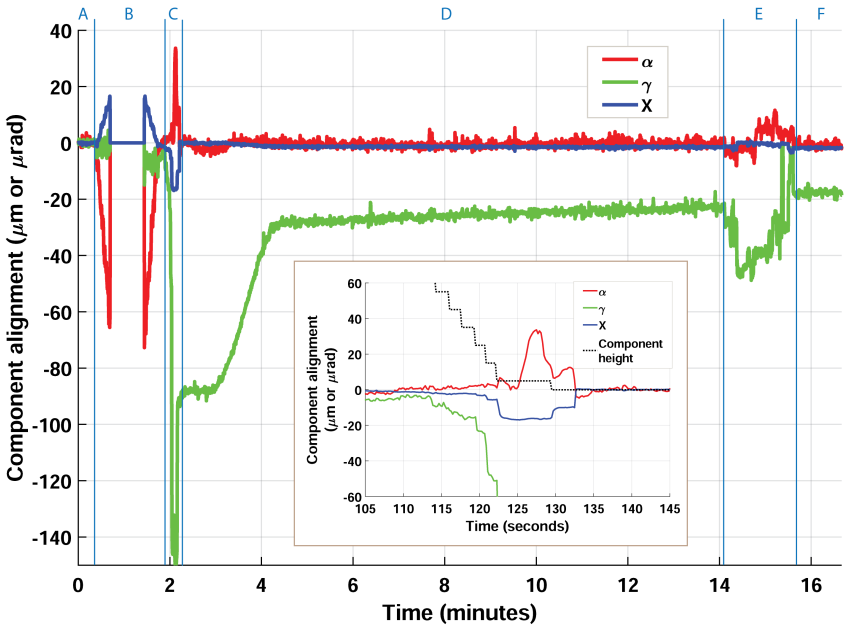

Fig. 7. Alignment information for the silicate test bond 5. The different stages of the bonding process are highlighted.
A: Angular alignment of the component bonding surface (β and γ) to the baseplate surface with the component held 200 μm above the baseplate.
B: Component lifted by 10 mm, bonding fluid deposited on the baseplate, and then an automated 'down to bond' sequence executed.
C: Bond fluid contact and spread followed by optimisation of component alignment α and X (also shown in more detail in inset).
C Inset: Detail of the bond fluid contact and spread. The bonding surface separation is reduced in 10 μm steps. At a separation of around 40 μm the component touches the bonding fluid. The size of the contact patch increases for the next few steps, causing alignment changes as the fluid pulls the surfaces together. The automated sequence stops at 122 seconds with full spread of the bonding fluid. A further 5μm step at 129 seconds is manually commanded, and reduces the misalignments. The final commanded alignment of the optical surface (α and X) occurs at 133 seconds after which the component is held in position without any further control inputs.
D: Initial bond development with component held in clamp; there are no control inputs during this period.
E: Release and retraction of the component clamp.
F: Continued bond curing and associated alignment development. The component is unconstrained and aligns itself to the baseplate as the bond cures. Long term development of the bond and alignment is shown in Fig. 8.

Optics EXPRESS

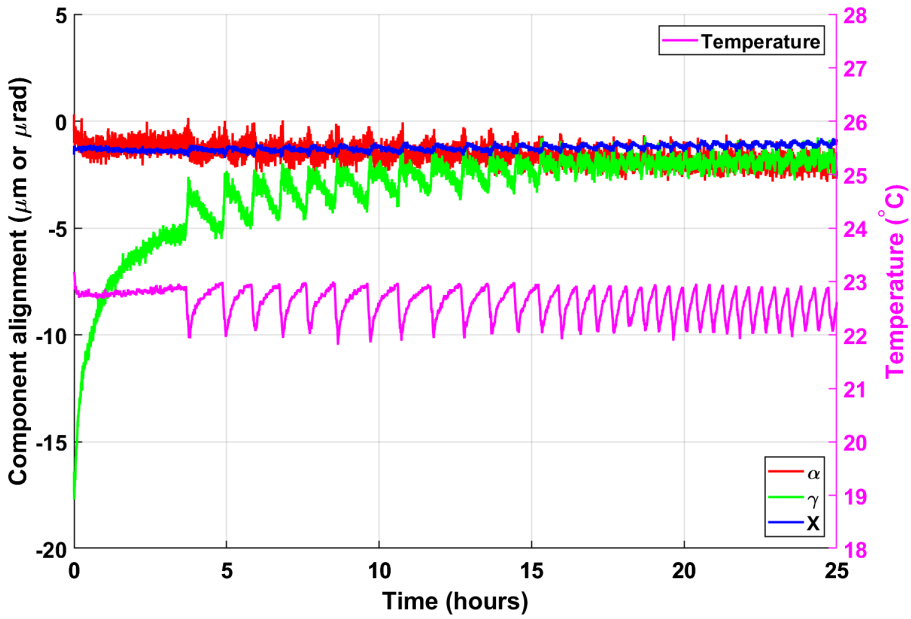

Fig. 8. Long term development of the alignment for silicate bond 5 after release from comonent holder. The data starts immediately after the component release shown as stage E in Fig. 7. Also shown is the room temperature. It can be seen that there is slight modulation of the γ angle of the bond by room temperature that decreases in amplitude as the bond approaches its final alignment.

5. Conclusions

We have demonstrated an automated alignment technique that allows us to consistently hydroxide catalysis bond optical components to within 4 μm and 10 μrad of their nominally desired alignment. The alignment technique uses an interferometric readout of the distance and angular alignment between the surfaces to be bonded, with the resulting signals used to provide feedback control that is implemented using a 6-axis micro-positioning hexapod. The time required to precision-bond an optical component using this new technique has been reduced by more than an order of magnitude compared with our previous manual approach. Bonding of a component can now be accomplished by a single operator in less than 30 minutes. We have also demonstrated that bonds made using a simple sodium hydroxide solution appear to offer further speed advantages during the curing stage, since they reach final alignment in a much shorter time than bonds made using the hydroxide solution with added sodium silicate. These advances open up new possibilities for efficient manufacturing of precision-aligned optical assemblies. They have particular relevance for space flight applications such as LISA, where the high-stability and high-strength of hydroxide catalysis bonds are particularly important.

Funding

UK Space Agency through an NSTP2 Technology Fast Track Project (contract number RP10G0348A220). We acknowledge support by the University of Glasgow, the UK Astronomy Technology Centre, and the Scottish Universities Physics Alliance.

Optics EXPRESS

References

1. C.W.F Everitt, D.B. DeBra, B.W. Parkinson, J.P. Turneaure, J.W. Conklin, M.I. Heifetz, G.M. Keiser, A.S. Silbergleit, T. Holmes, J. Kolodziejczak, M. Al-Meshari, J.C. Mester, B. Muhlfelder, V. Solomonik, K. Stahl, P. Worden, W. Bencze, S. Buchman, B. Clarke, A. Al-Jadaan, H. Al-Jibreen, J. Li, J.A. Lipa, J.M. Lockhart, B. Al-Suwaidan, M. Taber, and S. Wang, "Gravity Probe B: Final Results of a Space Experiment to Test General Relativity," Phys. Rev. Lett. **106**, 221101 (2011).
2. R.L Ward, R. Fleddermann, S. Francis, C. Mow-Lowry, D. Wuchenich, M. Elliot, F. Gilles, M. Herding, K. Nicklaus, J. Brown, J. Burke, S. Dligatch, D. Farrant, K. Green, J. Seckold, M. Blundell, R. Brister, C. Smith, K. Danzmann, G. Heinzel, D. Schutze, B. S. Sheard, W. Klipstein, D.E. McClelland, and D.A. Shaddock "The design and construction of a prototype lateral-transfer retro-reflector for inter-satellite laser ranging," Classical and Quantum Gravity **31**, 095015 (2014).
3. M. Armano, H. Audley, G. Auger, J.T. Baird, M. Bassan, P. Binetruy, M. Born, D. Bortoluzzi, N. Brandt, M. Caleno, L. Carbone, A. Cavalleri, A. Cesarini, G. Ciani, G. Congedo, A.M. Cruise, K. Danzmann, M. de Deus Silva, R. De Rosa, M. Diaz-Aguiló, L. Di Fiore, I. Diepholz, G. Dixon, R. Dolesi, N. Dunbar, L. Ferraioli, V. Ferroni, W. Fichter, E.D. Fitzsimons, R. Flatscher, M. Freschi, A.F. García Marín, C. García Marirrodriga, R. Gerndt, L. Gesa, F. Gibert, D. Giardini, R. Giusteri, F. Guzmán, A. Grado, C. Grimani, A. Grynagier, J. Grzymisch, I. Harrison, G. Heinzel, M. Hewitson, D. Hollington, D. Hoyland, M. Hueller, H. Inchauspé, O. Jennrich, P. Jetzer, U. Johann, B. Johlander, N. Karnesis, B. Kaune, N. Korsakova, C.J. Killow, J.A. Lobo, I. Lloro, L. Liu, J.P. López-Zaragoza, R. Maarschalkerweerd, D. Mance, V. Martín, L. Martin-Polo, J. Martino, F. Martin-Porqueras, S. Madden, I. Mateos, P.W. McNamara, J. Mendes, L. Mendes, A. Monsky, D. Nicolodi, M. Nofrarias, S. Paczkowski, M. Perreur-Lloyd, A. Petiteau, P. Pivato, E. Plagnol, P. Prat, U. Ragnit, B. Raïs, J. Ramos-Castro, J. Reiche, D.I. Robertson, H. Rozemeijer, F. Rivas, G. Russano, J. Sanjuán, P. Sarra, A. Schleicher, D. Shaul, J. Slutsky, C.F. Sopuerta, R. Stanga, F. Steier2, T. Sumner, D. Texier, J.I. Thorpe, C. Trenkel, M. Tröbs, H.B. Tu, D. Vetrugno, S. Vitale, V. Wand, G. Wanner, H. Ward, C. Warren, P.J. Wass, D. Wealthy, W.J. Weber, L. Wissel, A. Wittchen, A. Zambotti, C. Zanoni, T. Ziegler, and P. Zweifel "Sub-femto-g free fall for space-based gravitational wave observatories: LISA Pathfinder results," Phys. Rev. Lett. **116**, 231101 (2016).
4. M. Armano, H. Audley, J. Baird, P. Binetruy, M. Born, D. Bortoluzzi, E. Castelli, A. Cavalleri, A. Cesarini, A.M. Cruise, K. Danzmann, M. de Deus Silva, I. Diepholz, G. Dixon, R. Dolesi, L. Ferraioli, V. Ferroni, E.D. Fitzsimons, M. Freschi, L. Gesa, F. Gibert, D. Giardini, R. Giusteri, C. Grimani, J. Grzymisch, I. Harrison, G. Heinzel, M. Hewitson, D. Hollington, D. Hoyland, M. Hueller, H. Inchauspé, O. Jennrich, P. Jetzer, N. Karnesis, B. Kaune, N. Korsakova, C.J. Killow, J.A. Lobo12, I. Lloro, L. Liu, J.P. López-Zaragoza, R. Maarschalkerweerd, D. Mance, N. Meshksar, V. Martín, L. Martin-Polo, J. Martino, F. Martin-Porqueras, I. Mateos, P.W. McNamara, J. Mendes, L. Mendes, M. Nofrarias, S. Paczkowski, M. Perreur-Lloyd, A. Petiteau, P. Pivato, E. Plagnol, J. Ramos-Castro, J. Reiche, D.I. Robertson, F. Rivas, G. Russano, J. Slutsky, C.F. Sopuerta, T. Sumner, D. Texier, J.I. Thorpe, D. Vetrugno, S. Vitale, G. Wanner, H. Ward, P.J. Wass, W.J. Weber, L. Wissel, A. Wittchen, and P. Zweifel "Beyond the Required LISA Free-Fall Performance: New LISA Pathfinder Results down to 20μHz," Phys. Rev. Lett. **120**, 061101 (2018).
5. D. I. Robertson, E. D. Fitzsimons, C. J. Killow, M. Perreur-Lloyd, H. Ward, J. Bryant, A. M. Cruise, G. Dixon, D. Hoyland, D. Smith, and J. Bogenstahl, "Construction and testing of the optical bench for LISA Pathfinder," Classical and Quantum Gravity **30**, 085006 (2013).
6. A. A. van Veggel and C. J. Killow, "Hydroxide catalysis bonding for astronomical instruments," Advanced Optical Technologies **3** (2013).
7. E. D. Fitzsimons, J. Bogenstahl, J. Hough, C. J. Killow, M. Perreur-Lloyd, D. I. Robertson, and H. Ward, "Precision absolute positional measurement of laser beams," Appl. Opt. **52**, 2527–2530 (2013).
8. D. I. Robertson, E. D. Fitzsimons, C. J. Killow, M. Perreur-Lloyd, H. Ward, J. Bryant, A.M. Cruise, G. Dixon, D. Hoyland, D. Smith, and J. Bogenstahl "Construction and testing of the optical bench for LISA Pathfinder," Classical and Quantum Gravity, **30** 085006 (2013).